Asociación Argentina
de Mecánica Computacional

Mecánica Computacional Vol XXXI, págs. 2765-2781 (artículo completo)
Alberto Cardona, Paul H. Kohan, Ricardo D. Quinteros, Mario A. Storti (Eds.)
Salta, Argentina, 13-16 Noviembre 2012

RELIABILITY-BASED DESIGN OF A DYNAMICAL SUSPENSION WITH RANDOM STIFFNESS UNDER AN IMPOSED AMPLITUDE RESPONSE HULL

Emmanuel Pagnacco[a], Hafid Zidani[b], Rubens Sampaio[c], Eduardo Souza de Cursi[a] and Rachid Ellaia[b]

[a]*LOFIMS, EA 3828, INSA Rouen BP 8, 76801 Saint-Etienne du Rouvray, France, Emmanuel.Pagnacco@insa-rouen.fr*

[b]*LERMA, Mohammed V - Agdal University, Engineering Mohammadia School, Rabat, BP. 765, Ibn Sina avenue, Agdal, Morocco, ellaia@emi.ac.ma, hafidzidani@yahoo.fr*

[c]*PUC-Rio, Mechanical Eng. Dept. Rua Marquês de São Vicente, 225 22453-900 Rio de Janeiro RJ. Brazil, rsampaio@puc-rio.br*

Keywords: Structural dynamics, Mechanical design, Random systems, Uncertainty, Multi-objective optimisation, Pareto front, Reliability-based design optimisation.

Abstract. This paper deals with the design of a suspension, idealised as a spring-mass-damper system. The amplitude of a nominal system is constrained to satisfy certain limitations in a given frequency band and the design is to be done as a reliability-based optimisation. To concentrate in the main ideas, only the stiffness of the system will be considered random. The stiffness is characterised by a uniform random variable, and its mean and standard deviation are the optimisation parameters. The design problem is stated as a two-objective optimisation. The two-objective functions are the mean and the standard deviation of the stiffness. One searches for the lowest stiffness and the greatest standard deviation, while the amplitude response must be within the acceptable domain of vibration, which is prescribed.

To generate the Pareto front, the Normal Boundary Intersection (NBI) method is used in the RFNM algorithm. Results show that a not-connected Pareto curve can be obtained for some choice of constraint. Hence, in this simple example, one shows that difficult situations can occur in the design of dynamic systems when prescribing an amplitude-response hull. Despite the simplicity of the example treated here, chosen to highlight the main ideas without distraction, the strategy proposed here can be generalised for more complex cases and give valuable results, able to help designers to choose for the best compromise between the mean and the standard deviation in reliability-based designs.

1 INTRODUCTION

In this study, the design of a suspension is considered. It is idealised as a spring-mass-damper, having linear behaviour, leading to a simple single-degree-of-freedom (SDOF) dynamic system. The design parameter of interest is chosen to be the spring stiffness, while the design constraint consist in the prescription of a curve giving the acceptable amplitude response hull for the system responses over a given frequency range. That is, in the given frequency range the frequency response function (FRF) of the system, for any value of the stiffness, must be within the prescribed region.

Since uncertainty in the system is considered in this study, the design problem deals with random variables, in this case, to focus on the main ideas, only the stiffness of the system. More precisely, we chose to study the specific case of a bounded distribution for the stiffness, which leads us to consider a uniform distribution, a consequence of the Maximum Entropy Principle. Then, the stiffness can be characterised by its mean and standard deviation, which become the design parameters. Moreover, since the design is a reliability-based optimisation, one has to think now in terms of probability of acceptance for the design constraint. Thus, the acceptable probability of failure, specified by the designer, is an additional parameter of the problem.

To distinguish among the numerous design solutions, a vector objective function has to be defined, which leads to formulate an optimisation problem in its standard forms. Two scalar objective functions are chosen. One searches a suspension having the lowest mean stiffness, in order to keep low the cost of material, and the greatest standard deviation, in order to keep low the manufacturing costs. So the mean and the standard deviation of the random stiffness are the design objectives. This study has thus some similarities with previous studies on robust optimisation (Ritto et al., 2010, 2011).

Now it is described how the present study is organised: in the section 2, generalities of interest about the mechanical design are presented, when considering the reliability of the structures. The section 3 gives the equations of vibration to consider for the SDOF system, the adopted stochastic formulation and gives important results for the uncertainty propagation, which helps to link the probability of failure to the system random parameter. The section 4 specify the problem formulation for the reliability-based design optimisation. The section 5 shows three examples, one of them leads to a Pareto front which is unusual. The mechanical interpretation of the design for the vibration problem is throughly discussed.

2 GENERALITIES ABOUT THE MECHANICAL DESIGN WHEN CONSIDERING THE STRUCTURAL RELIABILITY

When a structure is loaded it deforms and develops internal stresses. This deformation and internal stresses must be within certain bounds which characterise the resistance of the material. That is, within the bounds the integrity and proper function of the structure are assured. Outside the bounds one says that the structure fails. The boundary between this two situations is known as the limit-state.

A simple example of ultimate limit-state is the Von Mises stress s compared to an acceptable resistance r of the structural material. Examples of serviceability limit-state can be a maximum deflection or an excessive vibration which do not exceed a human comfort threshold. Then, considering a continuous structure it is required to analyse not only one

spatial point of it but all points to ensure its design. To use standard Probability Theory, leads us to define a vector of limit states when adopting a spatial numerical description associated to a mesh of the mechanical part for a field.

Thus, the engineering task consists generally in finding the nominal design described by the set of parameters $\mathbf{x} \in \mathbb{R}^n$ which optimise an objective vector function $\mathbf{f} : \mathbb{R}^n \to \mathbb{R}^q$, subject to a vector failure criteria $\mathbf{g} : \mathbb{R}^n \to \mathbb{R}^m$. A typical formulation reads:

$$\begin{aligned} &\min_{\mathbf{x}} \left(\mathbf{f}\left(\mathbf{x}\right)\right) \\ &\mathbf{g}\left(\mathbf{x}\right) = \mathbf{r}\left(\mathbf{x}\right) - \mathbf{s}\left(\mathbf{x}\right) > \mathbf{0} \end{aligned} \tag{1}$$

where $\mathbf{s}$ is the load and $\mathbf{r}$ is the resistance, m denotes the number of control (spatial) points over the structure. However, the design solution which satisfy this formulation does not take into account uncertainties, which implies the possibility of undesirable structural responses in presence of them.

Thus, to handle structural or loading uncertainties it is preferable to think in terms of reliability when introducing a stochastic framework (Choi et al., 2007; Lemaire, 2009). In the sequel, the random variables are distinguished from the deterministic ones by denoting them in capital letters. Then, to deal with the uncertainties, we introduce an additional set of random processes $\mathbf{Y}$ which has to be consider in the structural design, and the structure will be considered unreliable if the failure probability of the limit-state exceeds a prescribed value. Limit-state functions $\mathbf{G}$ and probability of failure $\mathbf{P}_f$ are defined as:

$$\begin{aligned} &\mathbf{G}\left(\mathbf{x}, \mathbf{Y}\right) = \mathbf{R}(\mathbf{x}, \mathbf{Y}) - \mathbf{S}(\mathbf{x}, \mathbf{Y}) \\ &\mathbf{P}_f = \mathrm{Prob}\left[\mathbf{G}\left(\mathbf{x}, \mathbf{Y}\right) < \mathbf{0}\right] \end{aligned} \tag{2}$$

Both $\mathbf{R}$ and $\mathbf{S}$ are now functions of the nominal design variable $\mathbf{x}$ and the random processes $\mathbf{Y}$. The probability space to be used is $(\Omega, \mathcal{A}, P)$, where Ω is the set of sample space, $\mathcal{A}$ is an event space of subsets of Ω and P is a probability measure on $(\Omega, \mathcal{A})$.

The failure region is delimitated by $\mathbf{G} < \mathbf{0}$ while $\mathbf{G} = \mathbf{0}$ and $\mathbf{G} > \mathbf{0}$ indicate the limit state and safe region, respectively. The probability of failure is

$$\mathrm{Prob}\left[\mathbf{G}\left(\mathbf{x}, \mathbf{Y}\right) < \mathbf{0}\right] = \int \ldots \int_{\mathbf{G}(\mathbf{x},\mathbf{Y}) \leq \mathbf{0}} p_{\mathbf{Y}}\left(\mathbf{y}\right) \mathrm{d}\mathbf{y} \tag{3}$$

where $p_{\mathbf{Y}}$ denotes the joint probability density function of the limit-state function when considering all relevant random variables $\mathbf{Y}$. Note that the non-failure probability $\mathbf{P}_r$ is:

$$\mathbf{P}_r = 1 - \mathbf{P}_f \tag{4}$$

In the reliability problem it is also prescribed an admissible probability of failure, $\overline{\mathbf{P}}_f$.

3 FORMULATION OF THE STOCHASTIC VIBRATION PROBLEM

3.1 Equations for the vibration problem

Vibrations can often lead to undesirable results, such as discomfort or fatigue of passengers of a car whose suspension was not properly designed. Structural and mechanical

failure can often result from sustained vibration. In this study, we are interesting in designing a spring such that the one involves in the suspension device of a car or a motorbike. To limit vibration risk, specifications are set for the amount of vibration a device can withstand. Hence, in designing, it is of interest to adjust the physical parameters of the system in such a way that the vibration response meets the specified peak level given by the specification. Generally, a hull of acceptable peaks levels of vibration are established in the frequency domain and are express in terms of accelerations, but it can be express also in peaks displacements without difficulty.

This device is idealised in this study by as a simple linear spring-damper-mass system fixed at one end and subjected to an imposed harmonic displacement z at the other end (sketched on Figure 1). In the frequency domain, the displacement of this single degree of freedom (SDOF) system, u, is given by (Lin, 1967):

$$\left(k - m\left(2\pi f\right)^2 + \mathrm{j}2\pi f c\right) u\left(f\right) = q\left(f\right) \tag{5}$$

$$\text{with :} \qquad q\left(f\right) = m\left(2\pi f\right)^2 z\left(f\right) \tag{6}$$

where f is the frequency. In this equation, k, m and c are the stiffness, mass and damping system parameters (respectively), and the displacement $u\left(f\right)$ is obtained by solving equation (5), leading to :

$$u\left(f\right) = \frac{q\left(f\right)}{k - m\left(2\pi f\right)^2 + \mathrm{j}2\pi f c} \tag{7}$$

In contrast to a general mechanical problem which is continuous in the space dimension (as it is described in the previous section), this simple system has only one spatial degree of freedom.

To study this system, it is of interest to introduce the Frequency Response Function (FRF) $h\left(f\right)$ given by a unit forcing, leading to:

$$h\left(f\right) = \frac{1}{k - m\left(2\pi f\right)^2 + \mathrm{j}2\pi f c} \tag{8}$$

which has the amplitude:

$$\left|h\left(f\right)\right| = \frac{1}{\sqrt{\left(k - m\left(2\pi f\right)^2\right)^2 + \left(2\pi f c\right)^2}} \tag{9}$$

3.2 Stochastic formulation of the mechanical problem

This system becomes stochastic when the stiffness parameter or the loads (or both) are no longer deterministic. In the sequel, random variables will be denoted capitalising the letter that represents the deterministic variable, hence K and U in this case for the stiffness and the response amplitude.

The formulation adopted in this study is based on peak amplitudes of the system response. Considering the device has a random stiffness, the amplitude system response is a random process, which leads to study

$$U_K\left(f\right) = \frac{1}{\sqrt{\left(K - m\left(2\pi f\right)^2\right)^2 + \left(2\pi f c\right)^2}} \tag{10}$$

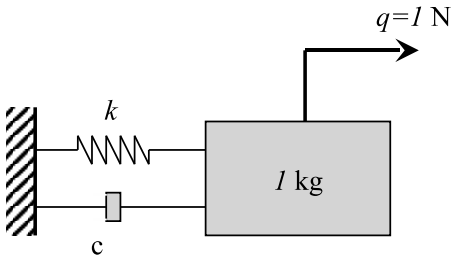

Figure 1: SDOF system.

for a unit forcing function. In addition, we chose to take a unit mass for numerical applications.

In this study, the probability law for the random variable K is chosen from the Maximum Entropy Principle (MEP) (Kapur and Kesavan, 1992; Rubinstein and Kroese, 2008). This principle states that the uniform probability maximises the entropy in the case of bounded domain of the random variable. Thus, the probability density function (PDF) given by the constant value $p_K(k) = \frac{1}{2\sqrt{3}\sigma_K}$ over $[\mu_K - \sqrt{3}\sigma_K, \mu_K + \sqrt{3}\sigma_K]$ is adopted for the random variable K, where μ_K denotes its mean value and σ_K its standard deviation. From the problem description proposed in the previous section, the set of random processes is $\mathbf{Y} = \{K; U(f)\}$ and the vector of design parameters is $\mathbf{x} = \{\mu_K, \sigma_K\}$. Note that μ_K has to be greater than $\sqrt{3}\sigma_K$ to ensure a positive stiffness while σ_K has to be non-negative.

From a design point of view, the amplitude of the vibration response has to respect the bound for the peak level given by the specification, at least within a chosen failure probability value $\overline{P}_f$. This define the limit state as:

$$\mathsf{G}(\mathbf{x}, \mathbf{Y}) = u_{\max}(f) - U_K(f) \qquad \text{for } f \in \mathcal{B} \tag{11}$$

where $u_{\max} : \mathcal{B} \to \mathbb{R}$ denotes the bound for the peak amplitude limit given by the specification and $\mathcal{B} = [0,\ f_{\max}]$.

3.3 Uncertainties propagation for the mechanical system

In our problem, the peak limit function $u_{\max}(f)$ is considered deterministic. Thus, we can write the non-failure probability as:

$$\text{Prob}\left[U_K(f) \leq u_{\max}(f)\right] = P_U(u_{\max}; f) \tag{12}$$

where P_U denotes the cumulative distribution function of the system amplitude response U_K at the fixed frequency f, thus:

$$\text{Prob}\left[U_K(f) \leq u_{\max}(f)\right] = \int_0^{u_{\max}(f)} p_U(u; f)\,\mathrm{d}u = \int_{u_{\inf}(f)}^{u_{\max}(f)} p_U(u; f)\,\mathrm{d}u \tag{13}$$

$p_U(u; f)$ being the probability density function (PDF) of the system and $u_{\inf}(f) = \inf\{u : p_U(u; f) > 0\}$ is the left endpoint of the support of P_U.

For a general problem, the distribution function of the system response amplitude is linked to the system random variables. Hence, considering a set $\mathbf{Z}$ of the system randoms variables and the system response function $U_{\mathbf{Z}}$, we have

$$P_U(u;f) = \int \ldots \int_{U_{\mathbf{Z}}(f)\leq u} p_{\mathbf{Z}}(\mathbf{z})\,\mathrm{d}\mathbf{z} \tag{14}$$

where $p_{\mathbf{Z}}$ is the joint PDF of variables $\mathbf{Z}$. Evaluating this expression is generally not straightforward, which necessitates to involve a numerical method, such as, for example, the Monte Carlo simulation method. In addition, to handle numerically the continuous limit state linked to the random processes set $\mathbf{Y}$, it is sampled at m fixed frequencies, leading to:

$$\mathsf{G}_j(\mathbf{x},\mathbf{Y};f_j) = u_{\max}(f_j) - U_K(f_j) \qquad \text{for } j\in[1,\ldots,m] \tag{15}$$

which are collected in the vector $\mathbf{G}$ of limit states, as it is done to handle limit states about mechanical space fields when considering static stresses or deformations of continuous solids. In such a case, the algorithm is:

1. Choose $\mathbf{x} = \{\mu_K,\ \sigma_K.\}$, $\mathcal{B} = [0,\ f_{\max}]$, and $u_{\max} : \mathcal{B} \to \mathbb{R}$;
2. Generate an event $K(\omega)$;
3. Compute $U_K(\omega)$: $\mathcal{B} \to \mathbb{R}$; that is, compute the displacement for the $K(\omega)$ generated in 2 solving the vibration problem;
4. For a sampling set of $\mathcal{B}$, $\mathcal{B}_m$, composed from m components, define the $\mathbf{Y_m}$ vector by $\{K; U_K(f), f\in\mathcal{B}_m\}$;
5. Define the function $G_j(\mathbf{x},\mathbf{Y_m})$ as the components of a $\mathbb{R}^m$ random vector;
6. Evaluate $P_U(u;f)$ from the Monte Carlo simulation method.

But for the problem considered in this study, there is only one single random variable K in the set $\mathbf{Z}$, and an analytical expression can be derived instead of using a Monte Carlo numerical simulation method. By using $p_U(u) = \frac{\mathrm{d}P_u}{\mathrm{d}u}$, it is found that (Zwillinger and Kokoska, 2000):

$$p_U(u) = \frac{1}{\left|\frac{\mathrm{d}U}{\mathrm{d}K}\right|_{k_1}} p_K(k_1) + \cdots + \frac{1}{\left|\frac{\mathrm{d}U}{\mathrm{d}K}\right|_{k_n}} p_K(k_n) \tag{16}$$

In this expression, k_j for $j = 1,\ldots,n$ denotes the roots of the algebraic equation $u(k,f) = u$, for f fixed (notice that $j = 1$ for a bijective function). This produces (Pagnacco et al., 2011):

$$p_U(u,f) = \begin{cases} \frac{1}{u\sqrt{u-(2\pi f c u)^2}} \times p_K(k) & \text{if} \quad u_{\inf}(f) \leq u(f) \leq u_{\sup}(f) \\ 0 & \text{if not} \end{cases} \tag{17}$$

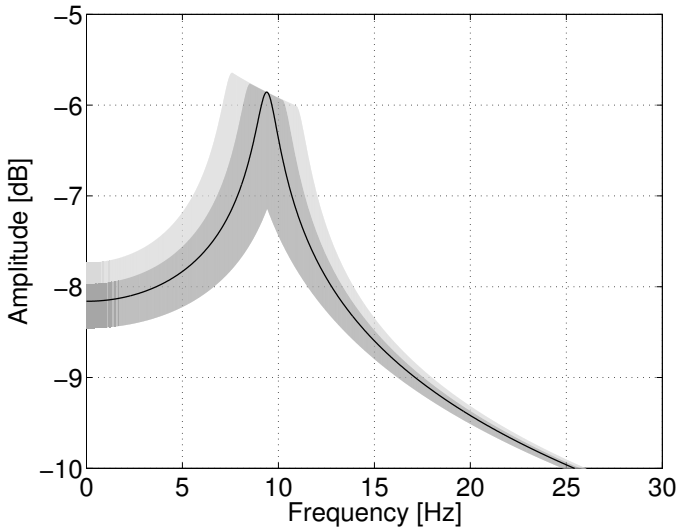

Figure 2: FRF amplitude of a SDOF system having a uniform distribution for the stiffness; thin line is for the nominal system response; grey region is for the total amplitude dispersion; light grey is for a probability greater than 75%.

where $u_{\sup}(f)$ denotes the upper envelope of the system response which is given by:

$$u_{\sup}(f) = \begin{cases} \frac{1}{\sqrt{\left(k_{\inf} - m(2\pi f)^2\right)^2 + 4\pi^2 c^2 f^2}} & \text{for } f^2 \in \left[0, \frac{k_{\inf}}{m}\right] \\ \frac{1}{2\pi f c} & \text{for } f^2 \in \left[\frac{k_{\inf}}{m}, \frac{k_{\sup}}{m}\right] \\ \frac{1}{\sqrt{\left(k_{\sup} - m(2\pi f)^2\right)^2 + 4\pi^2 c^2 f^2}} & \text{for } f^2 \in \left[\frac{k_{\sup}}{m}, +\infty\right[\end{cases} \tag{18}$$

and $u_{\inf}(f)$ denotes the lower envelope of the system response, given by:

$$u_{\inf}(f) = \begin{cases} \frac{1}{\sqrt{\left(k_{\inf} - m(2\pi f)^2\right)^2 + 4\pi^2 c^2 f^2}} & \text{for } f^2 \in [0, \mu_K] \\ \frac{1}{\sqrt{\left(k_{\sup} - m(2\pi f)^2\right)^2 + 4\pi^2 c^2 f^2}} & \text{for } f^2 \in [\mu_K, +\infty[\end{cases} \tag{19}$$

To illustrate these results, we chose a SDOF system having a mean of 3500 N and a standard deviation of 700 N. In the figure 2, the nominal amplitude in function of the frequency is plotted as well as the total dispersion, and a 75 % probability level.

4 FORMULATION OF THE RELIABILITY-BASED DESIGN OPTIMISATION PROBLEM

From a design point of view, an interesting objective is to design springs with the lowest stiffness in order to generate significant economical gains due to cheaper material. But another economical interesting point is to authorise a large dispersion about the nominal design when building multiple springs, that is do not be strict about the manufacture. Thus, the optimisation problem of interest is posed such as the one which minimise the mean stiffness μ_K and which simultaneously maximise its standard deviation σ_K, to reduce manufacture costs, leading to a bi-objectives optimisation problem ($q = 2$).

Consequently, the reliability based design optimisation problem has the following multi-objective form:

$$\begin{cases} \min \mathcal{F}(\mathbf{x}) & = (\mu_K, -\sigma_K)^{\mathrm{T}} \\ \text{subject to :} & \mathbf{P}_f = \mathrm{Prob}\left[u_{\max}(f_j) - U_K(f_j) < 0\right] \leq \overline{\mathbf{P}}_f, \\ & \qquad\qquad\qquad\qquad \text{for } j = 1, ..., m \\ & \mu_K > 3\sigma_K,\ \sigma_K \geq 0 \\ & K \sim \mathrm{Uniforme}(\mathbf{x}). \end{cases} \tag{20}$$

with the two-parameter vector $\mathbf{x} = \begin{bmatrix} \mu_K \\ \sigma_K \end{bmatrix}$ $(n = 2)$. Multi-objective optimisation involves the simultaneous optimisation of several incommensurable and often competing objectives. Since there is no preference information, a non-dominated set of solutions is obtained, instead of a single optimal solution. These optimal solutions are termed as Pareto optimal solutions. Stated in another way, Pareto optimal points are the solutions of the optimisation which cannot be improved in one objective function without deteriorating their performance in at least one of the other objectives. Hence, for a multi-objective problem the solution of the problem can be viewed as the Pareto front.

To generate the Pareto front, the Normal Boundary Intersection (NBI) method (Das and Dennis, 1998) is used to produce a series of constrained single-objective optimisations subproblems. The resulting optimisations subproblems are solved by using the Pincus representation formula in conjunction with Nelder-Mead algorithm and the penalty method which deals with the constraints produced by NBI. This leads to the RFNM optimisation algorithm (for Representation Formula Nelder-Mead), ables to find global optima for the Pareto front (Zidani et al., 2012).

The NBI first step is to find the solution sets x_i^* of q single-objective subproblems, corresponding to the individual global minima of each objectives $\mathcal{F}_i$, in order to build the vector $\mathbf{f}^*$ which contains the individual minima of the objectives (i.e., the utopia point). Next, NBI consists in making a sequential set of l single objective subproblems, which depends of a parameter $\mathbf{w}_l$ and defined by:

$$\begin{cases} \max\limits_{\mathbf{x},t} t \\ \text{subject to :} \quad \mathbf{\Phi}.\mathbf{w}_l + t.\mathbf{n} = \mathcal{F}(\mathbf{x}) - \mathbf{f}^*, \\ \qquad\qquad\ \ \mathbf{x} \in S. \end{cases} \tag{21}$$

where S is the admissible domain for the design-point solutions (the ones that satisfy all constraints), and:

- $\mathbf{\Phi}$ is the $q \times q$ pay-off matrix in which the i^{th} column is $\mathcal{F}(x_i^*) - \mathbf{f}^*$;
- $\mathbf{w}_l$ is a vector of chosen weights for the l-th subproblem and such that $\sum_{i=1}^{q} w_i = 1$, $w_i \geq 0$; and
- $\mathbf{n}$ is a quasi-normal direction which has negative components, i.e. it points towards the point $\mathbf{f}^*$ in the objective space $\mathcal{F}$. According to (Das and Dennis, 1998), it is chosen as $\pm\mathbf{n} = \frac{\mathbf{\Phi}.\mathbf{1}_q}{\|\mathbf{\Phi}.\mathbf{1}_q\|}$ where $\mathbf{1}_q$ is the all-ones column vector.

In subproblem (21), $\mathbf{\Phi}.\mathbf{w}_l$ defines a point on the so-called Convex Hull of Individual Minima (CHIM). The intersection between the normal $\mathbf{n}$ to the CHIM from the point and the boundary of the objective space $\mathcal{F}$ closest to the utopia is expected to be Pareto-optimal. The subproblem (21) depends of $\mathbf{w}$ which is the characterising parameter of the subproblem and its solution is referred as a NBI point. Solving it for l various distributed $\mathbf{w}_l$ enables to find distributed points on the boundary of $\mathcal{F}$, in order to construct a point-wise approximation of the efficient frontier. However, if the obtained set is not convex, NBI points are not necessarily Pareto-optimal points and a filtering has to be done *a posteriori* to obtain the true set of non-dominated points.

Following the RFNM procedure, each ($q+l$) constrained single-objective optimisation subproblem formed by the NBI methodology is then transformed into non-constrained optimisation subproblem by using the penalty methodology (Haftka and Gurdal, 1993). They are solved by using the Pincus representation formula (Pincus, 1970) in conjunction with the Nelder-Mead algorithm (Nelder and Mead, 1965; Haftka and Gurdal, 1993). In (Pincus, 1970) a Monte Carlo method for the approximate solution of some constrained optimisation problems is proposed, from which a representation formula has been expressed. It gives the optimum $\mathbf{x}^*$ of a single objective function $\mathcal{F}(\mathbf{x})$ defined on $\mathcal{S}$ as

$$\mathbf{x}^* = \lim_{\rho \to +\infty} \frac{\mathrm{E}\left[X.\exp\left(-\rho \mathcal{F}\left(X\right)\right)\right]}{\mathrm{E}\left[\exp\left(-\rho \mathcal{F}\left(X\right)\right)\right]} \tag{22}$$

where $\mathrm{E}[\bullet]$ denote the mean operator and X is a random variable vector taking its values on $\mathcal{S}$. In the RFNM procedure, the Pincus representation formula is used to obtain only a set of guess starting points $\mathbf{x}^{(0)}$ which are needed for the Nelder-Mead algorithm by generating only a small finite sample size of N pseudo-random numbers for the evaluation of the means. Using this solving strategy enables to find global optima. Note that it does not use sensitivities, that avoids drawbacks of the involved penalty methodology and makes it efficient.

5 APPLICATIONS

In this subsection, three applications are presented by considering two distinct amplitude peak response hull and two prescribe admissible failure probability, leading to significant differences in the Pareto-front solutions. In practice, sample size of $N = 50$ pseudo-random numbers are chosen for generating from the Pincus representation formula guess points $\mathbf{x}^{(0)}$ for the Nelder-Mead algorithm. Moreover, each optimisation run is repeated up to 10 times by using a new sample in order to ensure to find the global minima from the Nelder-Mead algorithm.

5.1 First two optimisation problems: choice of the hull and of two admissible failure probability

The first two optimisation problems are defined from the amplitude peak response hull that corresponds to the line segments delimited by points A to F given in the Table 1. The Figure 4 shows the prescribe amplitude peak response hull, as well as a FRF amplitude corresponding to a deterministic SDOF system which belongs to the permissible region, since it is entirely under the curve delimited by the prescribed hull. For this two problems, two distinct situations are investigated that corresponds to two probabilities of failure:

Points	A	B	C	D	E	F
Frequency [Hz]	0	3	9	13	16	29
Amplitude [dB]	-8	-5.5	-5.5	-6.45	-6.75	-10

Table 1: Coordinates of the points that define the amplitude peak response hull for the first and second optimisation problems.

Points	G	H	I	J	K
μ_K [N/m]	2981	4296	5957	6218	7142
σ_K [N/m]	0	1518	765	1518	3325

Points	G'	H'	I'	J'	K'
μ_K[N/m]	2981	4292	5983	6276	7194
σ_K [N/m]	0	757	378	757	1644

Table 2: Coordinates of characteristic points in the Pareto fronts (left for $\overline{P}_{f1} = 25\,\%$ and right for $\overline{P}_{f2} = 0$) for the first and second optimisation problems.

$\overline{P}_{f1} = 25\,\%$ and $\overline{P}_{f2} = 0$.

The Figure 3 exemplify the NBI method applied to the second problem by showing the construction of 21 distributed points on the boundary of $\mathcal{F}$. The points G' and K' are the first necessary two individual optima, G' being the minimum for $\mathcal{F}_1 = \mu_K$ and K' being the minimum for $\mathcal{F}_2 = -\sigma_K$. The point U' is the utopia. Next, the line segment G'K' plotted with a dashed line is divided into 20 subsegments. Then, each point on the boundary of $\mathcal{F}$, that are represented by a dot is found by maximising the normal distance from G'K', while constraints are satisfied. This corresponds to the subproblem (21).

However, for a better resolution in the applications, a set of 81 points is chosen to construct the boundary of $\mathcal{F}$. For each solution point on the NBI boundary front, since guess points for the Nelder-Mead algorithm comes from samples of random variables, the number of evaluations of the mechanical problem varies for each new run. For a relative stopping criteria of 10^{-4} in the evolution of the objective function or in the evolution of the parameters, it is observed that it varies from less than 100 evaluations to more than 800 evaluations. However, a histogram of 10,000 optimisation runs over the entire NBI front shows that it oscillates more frequently around two values, the first one being 100 evaluations and the second one being 400 evaluations.

Then, the RFNM optimisation procedure leads to the two NBI boundary fronts presented in the Figure 5. Although their values are different, they have similar shapes, which can be describe by 4 extremum points and an intermediate point, namely G, H, I, J and K for $\overline{P}_{f1}$ and G', H', I', J' and K' for $\overline{P}_{f2}$ in the Figure 5 and in the Table 2. Then, the interpretation of the optimal solutions and the explanation of their associated mechanical behaviour is common to the two Pareto fronts. Consequently, there is no need to distinguish the two situations in the following explanations, and we only discuss the front corresponding to $\overline{P}_{f1}$.

To conduct our explanations, we chose to travel along the NBI boundary front from the left point G to the right point K. The point G corresponds to the permissible minimal mean stiffness design: there is no solution design which can have a lower mean stiffness and do not exceed the peak response hull while satisfying parameters sides constraints (the positiveness for the design variables). At this design point, the stiffness standard deviation is also at its lowest value: it is zero. This is the limit situation where a random system becomes deterministic. So, there is no acceptable uncertainty at this design point. Hence,

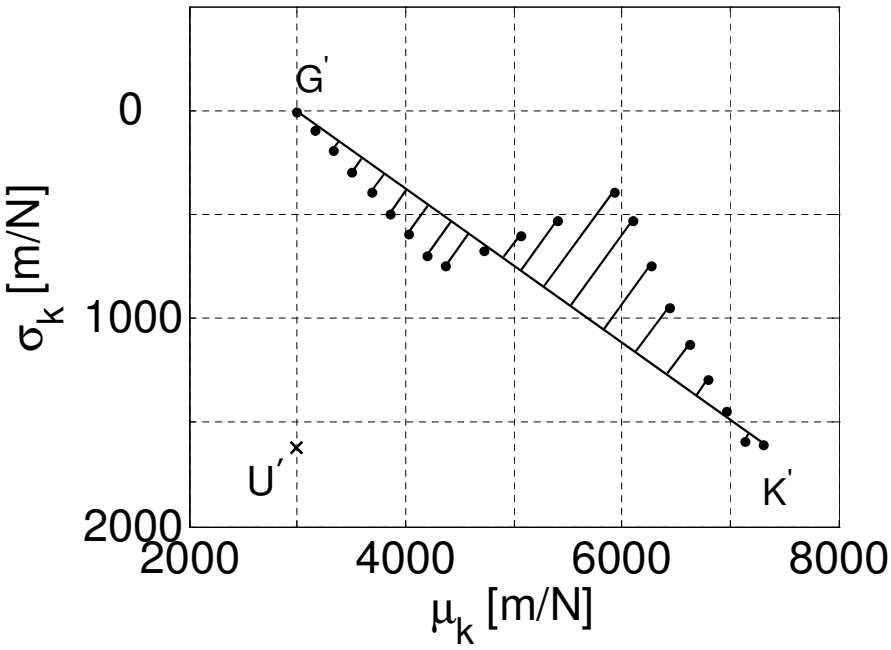

Figure 3: Construction of the NBI points for the second problem

we consider in this extreme situation that the failure probability constraint is respected for any target value. Observing the mechanical system response amplitude helps to better understand the design point G. In fact, the FRF amplitude shown in the Figure 4 is precisely the one of the mechanical system corresponding to this design point G. We can observe in this Figure 4 that the FRF amplitude intersects the available amplitude peak response hull at the null frequency[1]. It is clear from this figure that giving a non-null standard deviation would leads to a dispersion about the nominal response amplitude, which is impossible since there is no margins between the nominal response amplitude and the amplitude peak response hull at this (null) frequency. In addition, one can see that decreasing this optimal mean-stiffness value would increase the FRF amplitude over all frequencies, which is also impossible for the same reason. This explained the meaning of this solution.

On the contrary, increasing the mean stiffness results in a decrease in the amplitude response of the nominal system at all frequencies, thus also at the null frequency. This allows the nominal system to go away from the forbidden region delimited by the amplitude peak response hull, enabling now some randomness in the response. Thus, increasing the mean stiffness enables the increase of the stiffness standard deviation, as long as the failure probability is not exceeded. However, one has to keep in mind that increasing the mean stiffness increase also the resonant frequency of the system. So, by increasing the mean the optimal design solutions travels along the NBI front from the design point G to the design point H (Figure 5). However, the design point H is a limit situation where it becomes impossible to continue to increase the standard deviation by increasing the mean stiffness. At this design point H, the authorised system response dispersion (in the sense that it respect the constraint on the failure probability) is simultaneously constrained at

[1]The null frequency corresponds to a static loading.

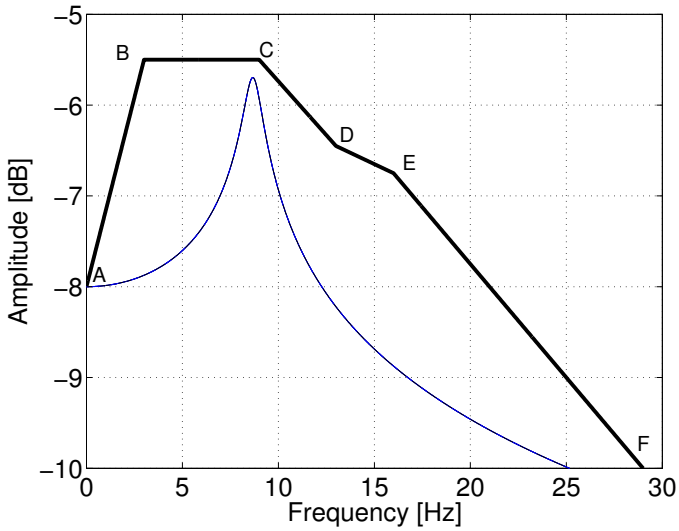

Figure 4: FRF amplitude of a deterministic SDOF system and the available amplitude peak response hull for the first problem

two distinct frequencies, namely 0 Hz and 12 Hz, as it is shown in the Figure 7. Thus, continuing now to increase the mean stiffness requires this time to decrease the stiffness standard deviation in order to respect the failure probability constraint. This takes the system from the design point H to the design point I in the front (note that these design solutions do not belongs to the Pareto front since both objectives functions are deteriorate when travelling through this way).

Then, coming on the design point I of the front, the achieved mean stiffness has leads to a sufficient decrease in the overall amplitude response, enabling the maximal amplitude response to go under the D-E segment of the amplitude peak response hull. This allows now an increase possibility in the standard deviation when increasing the mean stiffness, going from the design point I to the design point K in the front, when passing through the point J. This point J is the point which has the same standard deviation than the point H, but for a greater stiffness value. The last design point K in the front corresponds to the one that can has the greater standard deviation, which is the best design point when considering only this objective.

Through this analysis, it is clear that a filtering is necessary to extract the set of non-dominated points from the boundary front. When doing this, the resulting Pareto front is then constituted from two disjoints parts, namely the segments GH and JK for the first problem or G'H' and J'K' for the second problem (Figure 6).

5.2 Third optimisation problem: choice of the hull and one admissible failure probability

The last optimisation problem is defined from the amplitude peak response hull that corresponds to the lines segments delimited by points A" to F" given in the Table 3. Only the null failure probability is considered here, leading to the NBI boundary front of the Figure 8. Comparing Tables 1 and 3 shows that only the point D" differs from the point D between the previous and current optimisation problems. Consequently, the first part of the front of this third problem is common with the one of the previous problems, as we

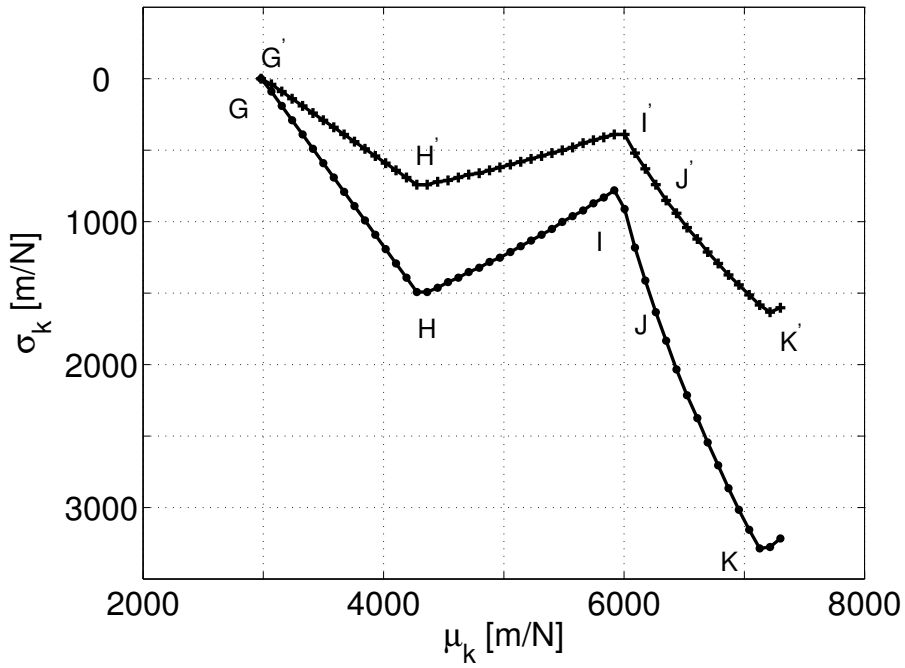

Figure 5: NBI boundary front for the first and second problems; the dot curve is for $\overline{P}_{f1} = 25\,\%$ and the other is for $\overline{P}_{f2} = 0$.

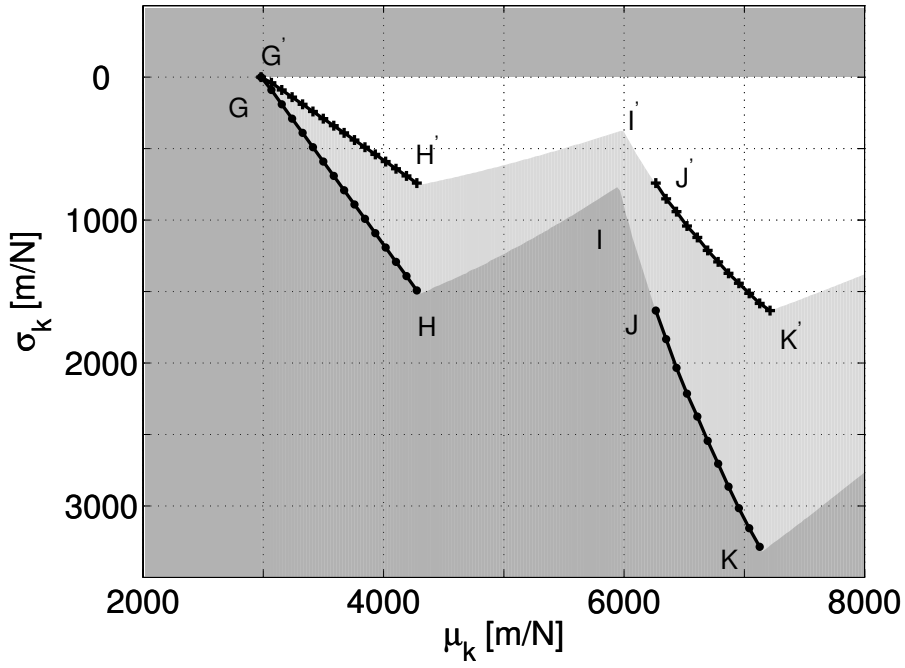

Figure 6: Pareto front for the first and second problems; the dot curve is for $\overline{P}_{f1} = 25\,\%$ and the other is for $\overline{P}_{f2} = 0$ and the grey region is for the not permissible domain (light grey is used for $\overline{P}_{f2} = 0$).

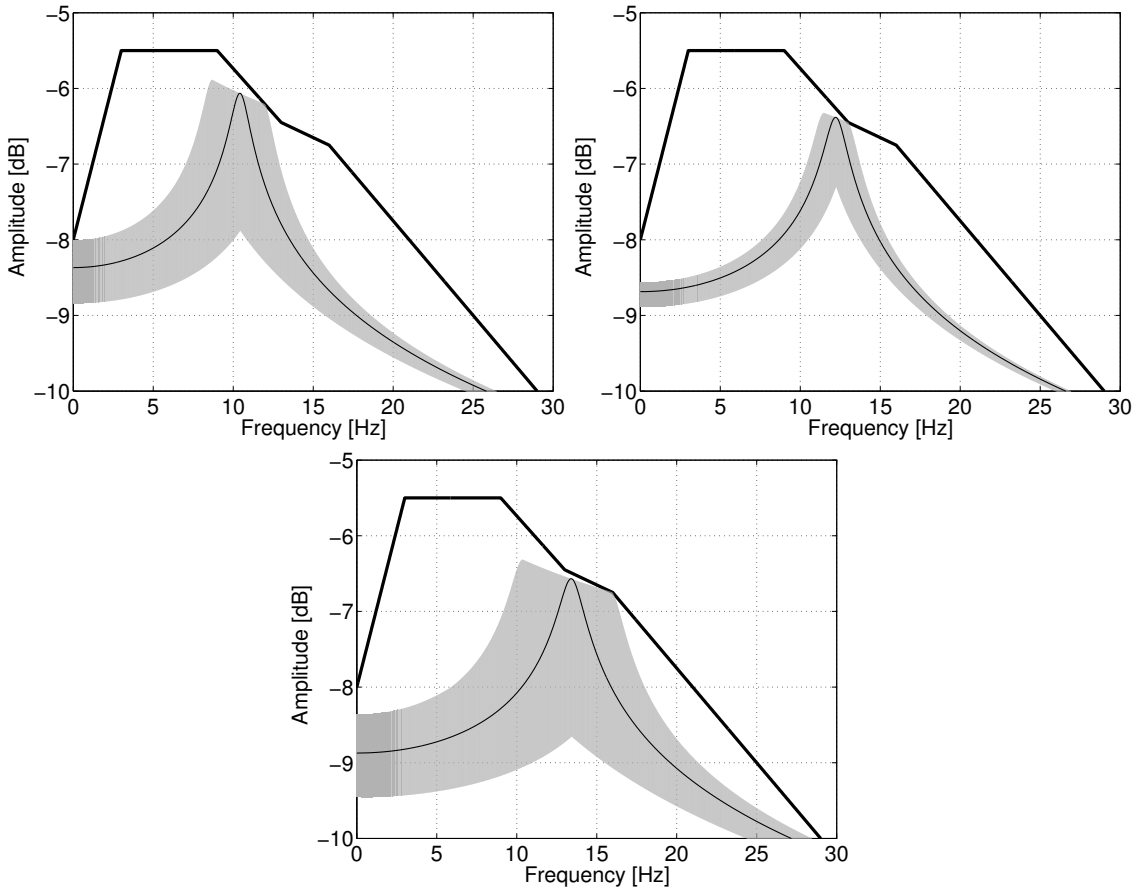

Figure 7: Graphs of the SDOF system FRF amplitude at the design points H (up, left), I (up, right), J (down). The grey region shows the dispersion that respect the failure probability constraint (i.e. the region corresponding to $P_f \leq \overline{P}_{f1}$), while the thin line indicates the response of the nominal system.

Points	A”	B”	C”	D”	E”	F”
Frequency [Hz]	0	3	9	13	16	29
Amplitude [dB]	-8	-5.5	-5.5	-6.52	-6.75	-10

Table 3: Coordinates of the points that define the amplitude peak response hull for the third optimisation problem

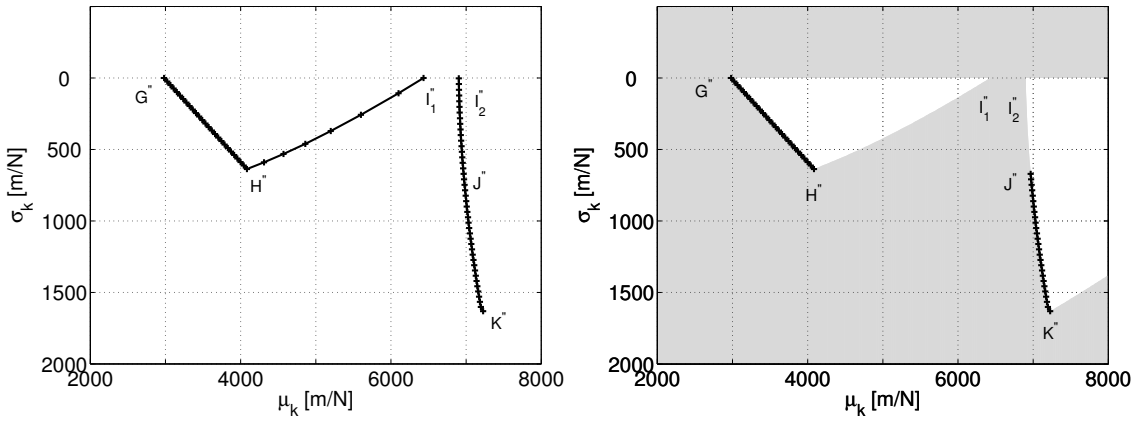

Figure 8: NBI boundary front (left) and Pareto front (right) for the third problem such that $\overline{P}_f = 0$.

can see in the Figure 8-left. However, there is a significant difference when approaching points $\mathrm{I}_1^{"}$ and $\mathrm{I}_2^{"}$, since there is no solution for the optimisation problem between $\mathrm{I}_1^{"}$ and $\mathrm{I}_2^{"}$. To understand why there is no admissible design here, the figure 9 shows the FRF amplitude of the SDOF system at these points. This situation leads to a not-connected front and occurs since there is no possibility for the FRF amplitude to have a peak resonance under the D” point of the amplitude peak response hull. In facts, even for a null standard deviation, the response level of the SDOF system is too high in this frequency range, when the mean stiffness takes values from 6434 to 6902 N/m.

As for the previous both problems, a filtering is necessary to find the Pareto front from the NBI boundary front, which leads finally to the segments G”H” and J”K” for this third problem (Figure 8-right).

6 CONCLUSIONS

A reliability-based design of a suspension is discussed in this study. The suspension is modelled as a SDOF dynamical system and the materials used as well as the manufacturing process constrain the stiffness to be bounded, for the sake of simplification and focusing on the main ideas, only the stiffness was considered random. The MEP gives the pdf of the stiffness as being a uniform distribution. A constraint to the problem is the prescription of a peak amplitude hull, that is a SDOF is only allowable if its FRF

Points	G”	H”	$\mathrm{I}_1^{"}$	$\mathrm{I}_2^{"}$	J”	K”
μ_K[N/m]	2981	4084	6434	6902	6961	7208
σ_K [N/m]	0	637.2	0	0	637.2	1639

Table 4: Coordinates of characteristic points in the Pareto front for the third optimisation problem.

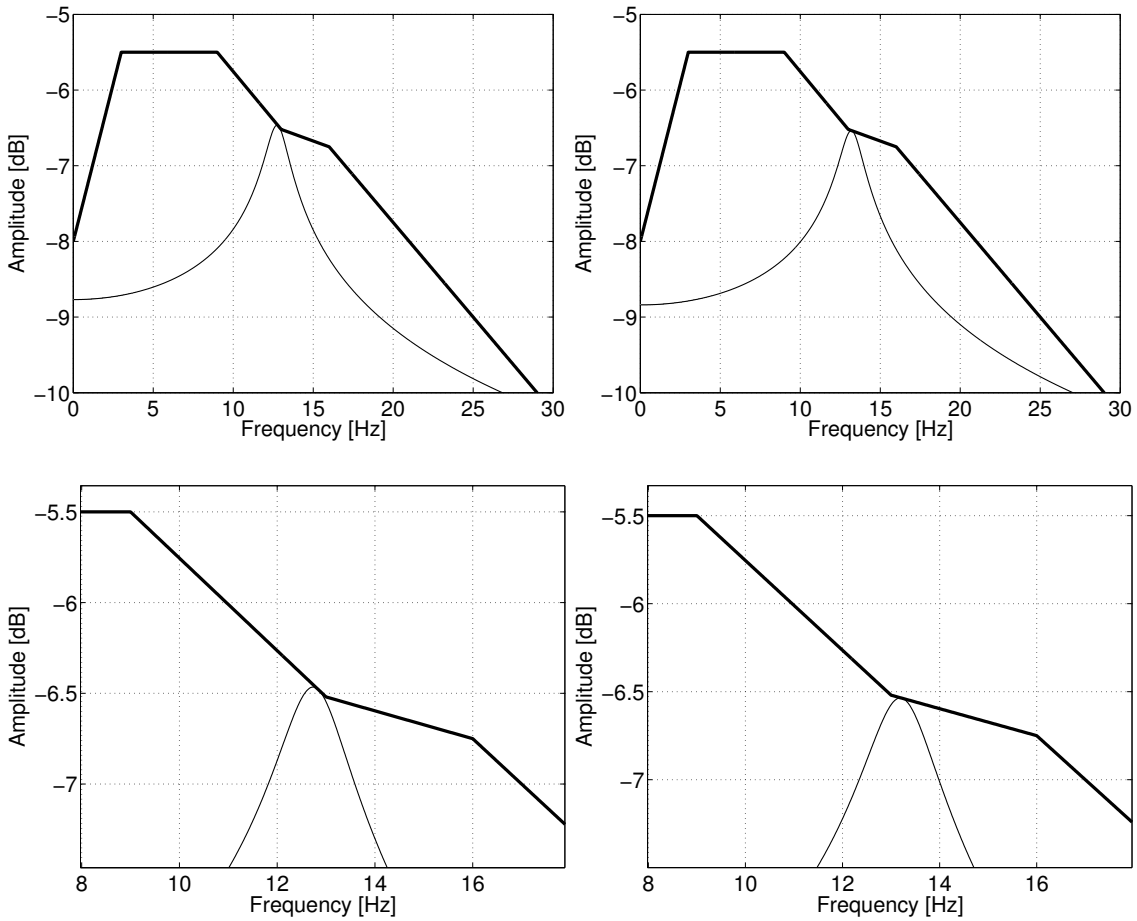

Figure 9: Graphs of the SDOF system FRF amplitude at the design points $\mathrm{I}_1^{"}$ (left) and $\mathrm{I}_2^{"}$ (right); bottom graphs are zoom of upper graphs.

amplitude, within the band of frequency of interest, stays within the region limited by the hull. Uncertainty propagation is achieved analytically in this situation. Since the design is reliability based, one must also prescribe a maximal acceptable failure probability, $\overline{P}_f$. The greater this probability, the less strict is the acceptance of the rules.

With this a multi-objective constrained reliability-based optimisation problem for the mean and the standard deviation of the stiffness is posed and the RFNM algorithm is used to solve the problem. Three examples are presented and explained mechanically, thanks to the analytical uncertainty results. It is shown that despite the simplicity of the modelling, a SDOF system, an interesting problem results and, for some choice of the constraint, a not-connected Pareto curve is obtained, meaning that there is a sub-frequency band where there is no solution for the problem, a result that to the best of the authors' knowledge appears for the first time in the literature.

REFERENCES

Choi S., Grandhi R., and R.A. C. *Reliability-based Structural Design*. Springer, 2007.

Das I. and Dennis J. Normal-boundary intersection: a new method for generating pareto optimal point in nonlinear multicriteria optimization problems. *SIAM Journal on Optimization*, 8(3):631–657, 1998.

Haftka R. and Gurdal Z. *Elements of Structural Optimization*. Kluwer Academic Publishers, Dordrecht, Netherlands, 1993.

Kapur J. and Kesavan H.K. *Entropy optimization principles with applications*. Academic Press, Inc., London, 1992.

Lemaire M. *Structural Reliability*. Wiley, 2009.

Lin Y.K. *Probabilistic theory of structural dynamics*. McGraw-Hill, Inc., New York, 1967.

Nelder J. and Mead R. A simplex method for function minimization. *Computer Journal*, 7:308–313, 1965.

Pagnacco E., Sampaio R., and Souza de Cursi E. Frequency response functions of random linear mechanical systems and propagation of uncertainties. *Mecanica Computacional*, XXX:3357–3380, 2011.

Pincus M. A Monte Carlo method for the approximate solution of certain types of constrained optimization problems. *Operation Research*, 18:1225–1228, 1970.

Ritto T., Holdorf R., Sampaio R., and Souza de Cursi J. Robust optimization of a flexible rotor-bearing system using the Campbell diagram. *Engineering Optimization*, 43(1):77–96, 2011.

Ritto T., Soize C., and Sampaio R. Robust optimization of the rate of penetration of a drill-string using a stochastic nonlinear dynamical model. *Computational Mechanics*, 45(5):415–427, 2010.

Rubinstein R.Y. and Kroese D.P. *Simulation and the Monte Carlo method*. John Wiley & Sons, Inc., New Jersey, USA, 2008.

Zidani H., Pagnacco E., Sampaio R., Ellaia R., and Souza de Cursi E. Multi-objective optimization by a new hybridized method: applications to random mechanical systems. *Engineering Optimization*, 44:to appear, 2012.

Zwillinger D. and Kokoska S. *Standard probability and statistics tables and formulae*. Chapman & Hall/CRC, New York, USA, 2000.